

OPEN ACCESS

A Critical Review of Using the Peukert Equation and its Generalizations for Lithium-Ion Cells

To cite this article: N. . Galushkin *et al* 2020 *J. Electrochem. Soc.* **167** 120516

View the [article online](#) for updates and enhancements.



A Critical Review of Using the Peukert Equation and its Generalizations for Lithium-Ion Cells

N. E. Galushkin,^{*,z} N. N. Yazvinskaya,^{id} and D. N. Galushkin^{id}

Don State Technical University, Laboratory of Electrochemical and Hydrogen Energy, Town of Shakhty, Rostov Region 346500, Russia

In this paper, the Peukert's equation was studied experimentally and theoretically at various discharge currents for lithium-ion cells. The classical Peukert's equation is not applicable at small discharge currents as according to this equation, at the discharge current decrease, the capacity released by the cells tends to infinity. The generalized Peukert's equation $C = C_m / (1 + (i/i_0)^n)$ corresponds well to the experimental data obtained at small and middle discharge currents. However at high discharge currents, the capacity released by the lithium-ion cells drops much faster than it is predicted by the known Peukert's equation generalizations. In this paper both experimentally and theoretically, it is proved that the reason of the sharp decrease of the cells capacity at high discharge currents is the voltage drop at cells internal resistance. Based on the obtained results, the following equation was proposed: $C = C_m(1 - i/i_1) / ((1 - i/i_1) + i^n/i_0^n)$. This equation corresponds well to the experimental data at any discharge currents, as it takes into consideration the voltage drop, caused by the cell internal resistance.

© 2020 The Author(s). Published on behalf of The Electrochemical Society by IOP Publishing Limited. This is an open access article distributed under the terms of the Creative Commons Attribution 4.0 License (CC BY, <http://creativecommons.org/licenses/by/4.0/>), which permits unrestricted reuse of the work in any medium, provided the original work is properly cited. [DOI: 10.1149/1945-7111/abad69]



Manuscript submitted February 10, 2020; revised manuscript received July 15, 2020. Published August 14, 2020.

At the present time, the lithium-ion type of batteries takes leading position in the segment of batteries of small-format.^{1,2} They are used for smartphones, notebooks, quadcopters, etc. However, in more recent times, the share of the lithium-ion batteries grows also in the segment of batteries of large-format. They are used in electric vehicles (xEV), in aviation, etc.²⁻⁵

Due to the batteries widespread use in various technical devices, their work is needed to be optimized. Notably, the optimization is necessary both on stage of technical devices designing and in the course of their operation.

The high-quality optimization achievement goal brings to necessity in develop reliable battery models. Currently, most fundamental models of batteries are built based on the fundamental electrochemical laws of ions and molecules transportation in porous electrodes and electrolyte. As a rule, a battery model is built with use of macro-homogeneous model of porous electrode.⁶⁻⁸ However, Hausmann in his paper⁹ showed that these electrochemical models of batteries are not applicable for electric vehicles (xEV) and aviation in view of a number of reasons.

Firstly, these models are very complicated and they cannot be solved by on-board computers of electric vehicles or airplanes.

Secondly, these models contain a lot of local parameters, measurement of which is hard or impossible. For example, it is impossible to measure various local parameters inside of a porous electrode.

Thirdly, in a case of batteries change in technical systems, the electrochemical models require new long-lasting calibration.

It should be also noted that many companies require such models creation, for which all the parameters would be measurable through experiments over the battery in whole without its dismantling. Models free of the above-mentioned shortages are impossible to be built based on the electrochemical method of modeling. Such models can be created only in frames of the statistical methods⁹⁻¹² or the non-linear structural methods of modeling.¹³ Usually, the statistical models are used when it is impossible or undesirable to use the electrochemical models^{9,10} or when the processes being under modeling are studied poorly (for example, thermal runaway,¹⁴⁻¹⁶ hydrogen accumulation in batteries electrodes,^{17,18} and gas generation during lithium-ion batteries cycling¹⁹⁻²¹).

Many statistical models are constructed on the basis of empirical equations. For example, in the paper⁹ in frame of a statistical model

development for evaluation of remaining capacity of lithium-ion batteries, the classical Peukert's equation was used, while in the paper,¹⁰ the improved Peukert's equation was applied. Hausman's model⁹ is specifically designed to evaluate the remaining capacity of batteries in electric vehicles. In electric vehicles, batteries operate in dynamic mode i.e. discharge currents can change quickly, and the temperature of the batteries must also be taken into account. In this model, the remaining battery capacity is calculated as the difference between the absolute capacity of a fully charged battery and the sum of the removed effective capacities over time periods $\Delta t = 1$ s. So, dividing the entire battery discharge time into the sum of small time intervals Δt allows us to consider (under dynamic load) that at each time interval Δt the current and temperature are constant. This makes it possible to use the empirical equations found for constant currents in Hausman's model. In this model, the discharged effective charges was found using the classical Peukert Eq. 1 (taking into account the temperature). The model was tested for commercial automotive-grade lithium batteries.⁹ The maximal relative error received under diverse discharge dynamical modes did not exceed 5%.

Also, the Peukert's equation can be used as the validation criterion of the fundamental electrochemical and structural models of batteries.

So even now, the Peukert's equation is widely popular. However, the classical Peukert's equation is not applicable at both very small and high discharge currents.²²⁻²⁴

This study is aimed at improvement of the classical Peukert's equation so that it would be applicable at any discharge currents.

Generalized Peukert's Equations

Most often, the Peukert's equation²⁵ is written as follows^{9,10}

$$C = \frac{A}{i^n}, \quad [1]$$

where C is capacity released by a battery at discharge current i , while A and n are empiric constants. The Eq. 1 is not applicable at small discharge currents as at discharge current decrease, the battery released capacity C will tend to infinity, which has no physical sense. It should be noted that there are other theoretical problems of applying Eq. 1, as well as Eq. 2, which follow from the analysis of the classical form of the Peukert equation and are discussed in detail in the paper.⁹

*Electrochemical Society Member.

^zE-mail: galushkinne@mail.ru

In our previous papers,^{10,22} it was proved experimentally that the generalized Peukert's equation

$$C = \frac{A}{1 + Bi^n}, \quad [2]$$

corresponds well to the available experimental data for both alkaline²² and lithium-ion¹⁰ batteries within the entire range of the discharge currents.

Rewrite Eq. 2 as follows

$$C = \frac{C_m}{1 + \left(\frac{i}{i_0}\right)^n}. \quad [3]$$

In this case at $i = 0$, we have $C = C_m$, i.e. C_m is the maximum capacity, which a battery is able to release. At $i = i_0$, we obtain $C = C_m/2$, i.e. i_0 is the current, at which the battery releases capacity twice less as compared to its maximum capacity. Thus, the constants in the Eq. 3 have the clear electrochemical sense unlike the Eq. 2, where A and B are merely empiric constants.

In the Fig. 1, the experimental data is given for the lithium-ion cell CGR18650E-Panasonic (2.2 Ah, LiNiCoO₂/Graphite) in comparison with the Eq. 1.

The curve of the classical Peukert's Eq. 1 is always concave (Fig. 1). That is why it can coincide with the experimental data for the lithium-ion cells only after the experimental curve inflection point, or at low discharge currents, where the experimental curve is concave. At small discharge currents, the experimental function $C(i)$ is concave in the range from zero to the value of the discharge current at which function $C(i)$ begins to decrease sharply Fig. 1(1). This range is various for different cells. It depends on the type of electrodes used, the design of the cells, their capacity, etc. This range of experimental values can be approximated by the classical Peukert Eq. 1 with high accuracy. For the Panasonic-CGR18650E cells (Table I), the classical Peukert Eq. 1 with high accuracy corresponds to the experimental data in the range of discharge currents from 0.1C_n to 2 A (Fig. 1(1)), and for the Samsung-INR18650-13Q cells in the range from 0.1C_n to 15 A. It should be noted that for the Samsung-INR18650-13Q cells, the range of the discharge currents, where the classical Peukert Eq. 1 is applicable, covers the entire range of operating currents of these cells. Therefore, for these cells, the classical Peukert Eq. 1 can be used in any models in the field of operating currents. Also for commercial automotive-grade lithium-ion batteries, the classic Peukert equation is true in the range of discharge currents, which covers the entire range of operating currents of these batteries. That is why in the Hausman's model,⁹ the classic Peukert equation (taking into account the temperature) is successfully used to estimate the remaining capacity of these batteries.

The generalized Peukert's Eq. 3 corresponds well to the experimental data at the small and middle discharge currents. However at the very high discharge currents, the Eq. 3 differs considerably from the experimental data. It is seen especially clearly in the logarithmic coordinate system (Fig. 2).

Consider the reason why the faster drop of the cell released capacity can be going on at the discharge current growth, than the Eq. 3 predicts it. With this purpose in mind, investigate the connection between the empiric Peukert and Shepherd equations.

Like the Peukert's equation, the Shepherd's one²⁶ is one more empiric equation among the most well-known ones describing the process of the battery discharge:

$$U = E - Ri - K \left(\frac{C}{C_m - C} \right) i + u_r \left[\exp \left(-B \frac{C}{C_m} \right) - 1 \right], \quad [4]$$

where U is voltage on battery terminals, C is battery released capacity, i is discharge current, R , C_m is internal resistance and battery maximum capacity, E is electromotive force (EMF) of a fully

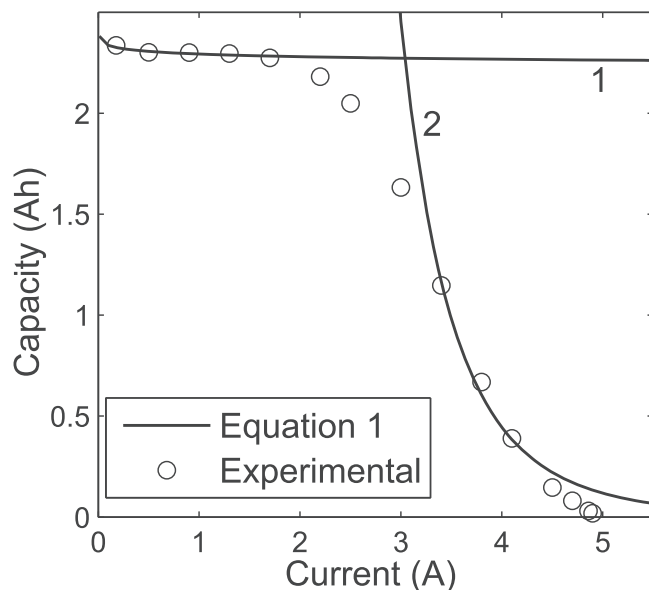


Figure 1. Comparison of experimental data with Peukert's Eq. 1 for lithium-ion cell CGR18650E-Panasonic. Number 1 marks the Peukert equation at small discharge currents, and number 2 at high discharge currents.

charged battery, u_r is voltage drop due to relaxation processes in discharge process beginning, K and B are empiric constants.

Consider a battery discharge at the constant current i up to the final voltage u_k , which is determined by the batteries' producer. For the parameters of the Eq. 4 in the end of the discharge process, we shall have the following equations

$$U = u_k, \quad u_r \left[\exp \left(-B \frac{C}{C_m} \right) - 1 \right] \approx -u_r. \quad [5]$$

The validity of the second Eq. 5 is evident as the relaxation processes connected with the discharge process inclusion fade out completely by the end of the battery discharge.

Use if a battery is discharged by a small current, it is possible to pay no regard to the voltage drop, caused by the cell internal resistance, i.e. $Ri \approx 0$. In this case, from the Shepherd's Eq. 4 (taking into account Eq. 5) for battery released capacity, we obtain the equation

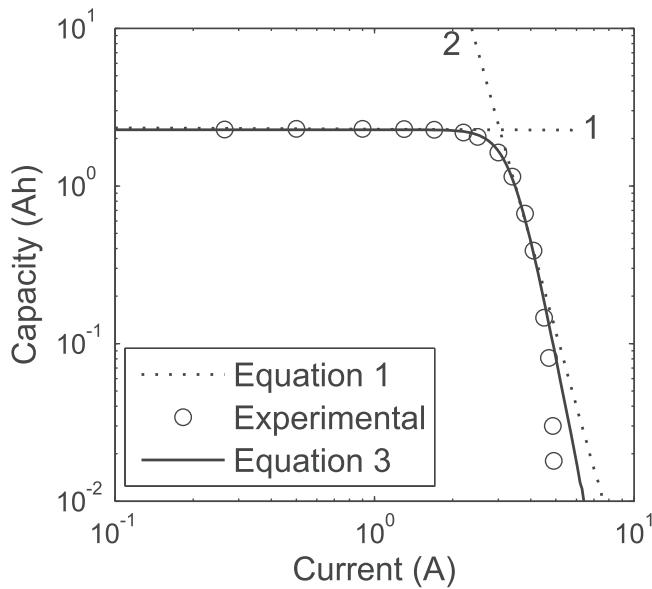
$$C = \frac{C_m}{1 + Di}, \quad \text{where } D = \frac{K}{E - u_k - u_r} \quad [6]$$

The Eq. 6 is the well-known Liebenow's equation.²⁷ Following the Peukert's equation, the Liebenow's empiric equation was proposed for the lead-acid battery capacity calculation at small discharge currents, at which the Peukert's equation was inapplicable. Indeed, the Eq. 6 describes well the released capacity of lead-acid batteries at small discharge currents.²⁶ However in the range of the middle discharge currents, the Peukert's equation is valid (virtually for batteries of all the electrochemical systems).^{9,10,22} In our previous papers^{10,22} experimentally, it was proved that for the alkaline and lithium-ion batteries at the small and average discharge currents, the generalized Peukert's Eq. 3 is valid.

It should be noted that the Shepherd's Eq. 4 like the Liebenow's and Peukert's ones was firstly obtained for the lead-acid batteries.²⁶ So there is no surprise that the empiric equations by Shepherd and Liebenow are connected tightly. Currently, the Shepherd's Eq. 4 is used also for the discharge analysis of batteries of other electrochemical systems.^{9,28} However from the above-conducted analysis, it follows that the Shepherd's equation (likewise the Liebenow's equation) is valid only at the small discharge currents. In the paper,¹³ this fact was confirmed both experimentally and theoretically. In

Table I. Characteristics and parameters for the initial cycles of the investigated commercial lithium-ion cells.

No. of the Cell	1	2	3
Model	CGR18650E	AMP20M1HDA	INR18650-13Q
Manufacturer	Panasonic	A123	Samsung
Cathode material	LiNiCoO ₂	LiFePO ₄	LiNiMnCoO ₂
Capacity (Ah)	2.2	20.0	1.3
Charge current (A)	1.25	10	0.75
Upper cutoff (V)	4.2	3.6	4.2
End-current (mA)	50	500	50
Discharge current (A)	0.5	5	0.5
Lower cutoff (V)	3	2.0	2.5

**Figure 2.** Comparison of experimental data with Peukert's Eqs. 1 and 3 for lithium-ion cell CGR18650E-Panasonic in logarithmic system of coordinates. Number 1 marks the Peukert equation at small discharge currents, and number 2 at high discharge currents.

order to make the Shepherd's equation valid at average discharge currents, too, it is needed to change it so that—after the retransformation (Eq. 5)—from it, the generalized Peukert's equation could be obtained (Eq. 3). In this case, the Shepherd's Eq. 6 will take the following form

$$U = E - Ri - K \left(\frac{C}{C_m - C} \right) i^n + u_r \left[\exp \left(-B \frac{C}{C_m} \right) - 1 \right], \quad [7]$$

Based on the macro-homogeneous model of porous electrode¹³ (and the experimental studies), our theoretical calculation showed that the generalized Shepherd's equation must look exactly like the Eq. 7 at the small and average discharge currents. At $n = 1$ from the Eq. 7, we obtain the classical Shepherd's equation, which is valid only for the small discharge currents.¹³

If to use the Eq. 7 with the due account of the Eq. 5, for the dependence of the battery capacity on the discharge current, we shall obtain the generalized Peukert's Eq. 3. If in addition to take into account also a battery internal resistance, we'll obtain the following equation:

$$C = \frac{C_m(1 - i/i1)}{(1 - i/i1) + \left(\frac{i}{i0}\right)^n} \quad \text{where} \quad [8]$$

$$i0 = \sqrt[n]{\frac{E - u_k - u_r}{K}} \quad \text{and} \quad i1 = \frac{E - u_k - u_r}{R}$$

The Eq. 8 differs from the generalized Peukert's Eq. 3 as it has the additional multiplier $(1 - i/i1)$. This multiplier takes into consideration the voltage drop, caused by the cell internal resistance. At $i = i1$, the battery released capacity will be equal to zero. Hence, at the discharge current $i = i1$ already at the moment of the battery discharge start, on the battery terminals, there will be observed the final discharge voltage, i.e. $U = u_k$. Such situation is quite possible at the high discharge currents with due taking into consideration the voltage drop on the battery internal resistance.

So the conducted by us analysis shows that if to take the battery internal resistance into consideration, the capacity released by it must drop faster at the high discharge currents than it follows from the Peukert's Eqs. 1 and 3.

In conclusion, we note the following useful equation

$$\lim_{i \rightarrow i1} \frac{d}{di} C(i) = -C_m \left(\frac{i0}{i1} \right)^n \frac{1}{i1} \quad [9]$$

From the Eq. 9, it is seen that at a discharge current growth, the curve $C(i)$ comes to the point $C(i1) = 0$ under a negative angle, the value of which depends on all the parameters characterizing the Eq. 8.

The fact that the Peukert's Eq. 1 is not applicable at the high discharge currents was observed by other authors, too. For example, in the paper,²³ the following improved Peukert's equation was proposed

$$C = \frac{A}{i^n} \sqrt{\frac{1}{s1^{(i/s2-1)} + 1}}, \quad [10]$$

which correctly describes the discharge of the lithium-ion batteries at the high discharge currents. In the Eq. 10, $s1$ and $s2$ are the new empirical constants. The additional multiplier was entered into the Eq. 10, which is similar to the use of such multiplier in the radiotechnics for determination of the cut-off frequency of the low-pass filters. It can be said about the Eq. 10 that from the formal point of view, it is able to describe the dependence $C(i)$ at any discharge currents correctly. However in no way, this empiric equation can explain a reason of such sharp decrease of the batteries capacity at the high discharge currents.

Experimental

For a verification of the generalized Peukert's Eqs. 3 and 8, there were used the commercial lithium-ion cells of different formats and capacities, and made by different manufacturers (the manufacturers,

models, nominal capacities and cathode material of the studied batteries are presented in Table I).

The cells were cycled according to their operation manuals. The charge procedure consisted in the constant current and constant voltage (CC/CV) application. The discharge procedure consisted in application of constant current (CC). The parameters and criteria of the cells charge and discharge (for initial cycles) are represented in the Table I.

For cell cycling, a ZENNIUM electrochemical workstation with a PP241 potentiostat (ZAHNER-elektrik GmbH & Co. KG, Kronach, Germany) was used (accuracy: voltage $\Delta U = \pm(0.1\%$ of reading), current $\Delta I = \pm(0.25\%$ of reading)). Additionally, when discharging AMP20M1HDA cells by high currents, an electronic load (custom-made) with a maximum input current of 430 A was used (accuracy: current $\Delta I = \pm(0.25\%$ of reading)). The electronic load was connected to the ZENNIUM workstation using an analog-to-digital converter (based on MAX1272 from Maxim Integrated).

The temperature of the cells was measured using an LM35 temperature sensor fixed to the side of the cells (accuracy $\Delta T = \pm 0.2\%$ of reading ($^{\circ}\text{C}$)).

For the purposes of heat exchange and cooling intensity increase, when the cells were discharged by high currents, modified heat sinks were fastened to them (usually used for computer processor cooling). Their fixation was done with the aid of heat-conducting paste MX-2 (ARTIC) and a specially manufactured clamp (Fig. 3). For prismatic pouch cells AMP20M1HDA (Table I), two heat sink PR169/10/SE were used, which were attached on different sides. As a result, the temperature of the cells in all our experiments was well below 55°C .

Nickel strips were attached to the center of each electrode of cylindrical lithium-ion cells by laser welding. Then the wires from the PP241 potentiostat were attached to the nickel strips using screw clips. In the case of prismatic pouch cells AMP20M1HDA (Table I), wires from the PP241 potentiostat were connected to the terminals using powerful screw clamps.

The cells were cycled inside of the climatic chamber Binder MK240 (BINDER GmbH, Germany). To discharge the cells, the potentiostat was connected to the cells with wires through specially made holes in the climate chamber, which were then sealed.

The experimental studies of the cells were performed in accordance with the following steps.

Firstly, preliminary on each cell, not less than ten initial cycles were executed for their parameters stabilization in connection with the layer SEI formation. The initial cycles were performed in accordance with the parameters and criteria specified in the Table I. The initial cycles stopped when, in three cycles in line, the cell released capacities differed from each other by less than 5%.

Secondly, in the measurement cycles, the cells were charged in accordance with the parameters given in the Table I.

The discharge currents ranged from $0.2 C_n$ up to the currents, at which the cell released capacity was close to zero. As the released capacity at certain values of discharge current, the average capacity values obtained in three charge-discharge cycles without interruption were taken. However if in these three cycles, the released capacity differed more than by 5%, additional initial cycles were executed and the experiment was repeated again (or the cell was exchanged by another more stable cell, and the experiment was performed from the very beginning).

Thirdly, in order to prevent a mutual influence of the charge-discharge cycles (through various residual phenomena), before each change of the discharge current or the cell temperature, the initial cycles were performed. The initial cycles were executed until the difference from each cycle was less than 5% in three cycles in line.

In the first group of the experiments, we explored the cell temperature influence on the cell released capacity. The cells were cycled inside of the Binder MK240 climatic chamber (Binder GmbH, Germany). The measurements were performed in the initial cycling mode (Table I). Since the discharge current in this group of experiments is small, the cell temperature almost did not differ from

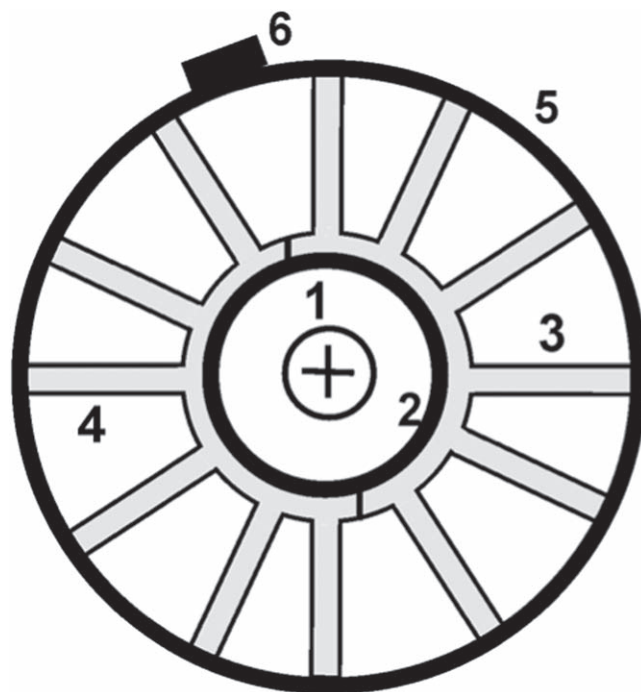


Figure 3. Drawing of the setup (top view): (1) lithium-ion cell, (2) heat-conducting paste, (3, 4) two halves of a modified heat sink, (5) clamp, and (6) screw of the clamp.

the temperature set in the climatic chamber. However, the cell temperature was controlled by a temperature sensor. Before testing at a certain temperature, the cell was kept at this temperature for at five hours in order to fully reach the desired temperature inside the cell. Measurements were performed in the temperature range from 263 to 328 K. The temperatures for measurement were selected in a random sequence from the studied range. Before each change in the measurement temperature, as a rule, from three to five initial cycles were performed (at a temperature of 298 K), before stabilization of the released cell capacity within 5%. This leads to the fact that the initial state of the cell after stabilization, is the same before any new measurement.

In the second group of experiments, we studied the influence of the discharge current on the cell released capacity. The general scheme of the measurement cycle consisted of the following stages. The first stage, the cell charge in the standard mode in accordance with the parameters and criteria given in the Table I. The second stage, the discharge of the cell by current from the studied range from $0.2 C_n$ up to the currents, at which the cell released capacity was close to zero. This charge-discharge procedure was repeated three times and the average value of the released cell capacity for this discharge current was found. The third stage, then, as a rule, from three to five initial cycles were performed, before stabilization of the released cell capacity within 5%. Then these three stages were repeated again, but with a new discharge current, etc. to the end of all measurements.

It should be noted that when using the initial cycles to stabilize the released cell capacity within 5%, the sequence of discharge currents is of little importance. This experimental fact follows from the fact that the initial state of the cell, after stabilization, is the same before any discharge current. Therefore, we performed a discharge of cells in a random sequence of currents from the studied range.

Results

The cell released capacity depends on two external parameters, which are the discharge current and the cell temperature.^{9,10}

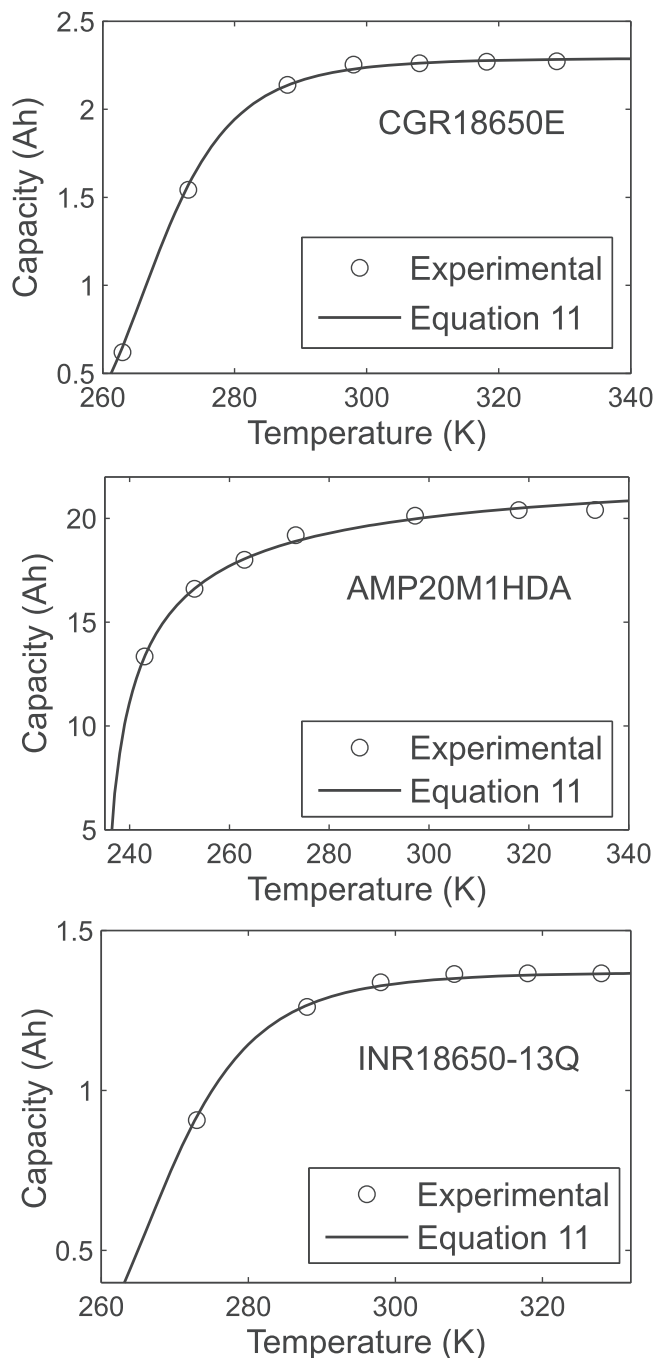


Figure 4. Dependence of cell released capacity on cell temperature at discharge currents from Table I.

Dependence of the released capacity on the cell temperature.—

In the first group of the experiments, we explored the cell temperature influence on the released capacity. These measurements were performed in accordance with the general measurements scheme, for this group of experiments, described in the experimental section. The results of the experimental investigations are given in the Fig. 4.

In the paper,¹⁰ it was proved experimentally that the dependence of the cell released capacity on the cell temperature adheres to the empiric equation

$$C = C_{mref} K \frac{\left(\frac{T - T_L}{T_{ref} - T_L} \right)^\beta}{(K - 1) + \left(\frac{T - T_L}{T_{ref} - T_L} \right)^\beta} \quad [11]$$

where C_{mref} is the maximum capacity released by a cell at the temperature T_{ref} ; T_L is the temperature, at which $C = 0$, i.e. this is the temperature close to one of the electrolyte freezing, when all the electrochemical processes would stop; and T_{ref} is the reference temperature for the studied type of the cells. From the Eq. 11, it follows that at $T = T_{ref}$, the temperature-related multiplier is equal to 1, i.e. it does not make any impact on a cell capacity. Nevertheless, in a case, when $T \rightarrow \infty$, the temperature-related multiplier in the Eq. 11 will tend to the parameter K . So, the parameter K shows how many times (theoretically) the capacity C in the Eq. 11 can be increased with a cell temperature growth in comparison of the capacity C_{mref} .

The optimal parameters for the Eq. 11 were found based on the least square method with use of the Levenberg–Marquardt optimization procedure. The obtained optimal parameters are given in the Table II. The reference temperature for the studied cells is $T_{ref} = 298$ K.

From the analysis of Fig. 4, it is seen that in the temperature range 298–328 K, the cell released capacity changes insignificantly at all. The relative deviation of the capacity from the average value in this temperature range is less than 1%. Hence, the temperature impact can be neglected, while studying the dependence of the cell released capacity on the discharge current in this temperature range.

Dependence of cell released capacity on discharge current.—In the second group of experiments, we studied the influence of the discharge current on the cell released capacity.

These measurements were performed in accordance with the general measurements scheme, for this group of experiments, described in the experimental section. The use of the heat sink allowed limiting a temperature increase of the cells at their discharge process by the high currents. The temperature limitation was achieved due to the considerable improvement of the heat exchange with the ambient environment and the use of the climatic chamber. So in all our experiments, the cell temperature didn't exceed 328 K. Therefore, in accordance with the studies in the previous section, the effect of temperature on the cells released capacity was negligible. It should be noted that all the cells under investigation had no protection, so it was possible to discharge them with the high currents.

The obtained experimental data for the cells under investigation (Table I) are represented in the Fig. 5.

For the Peukert's generalized Eqs. 3 and 8, the optimal parameters were found based on the least square method with use of the Levenberg–Marquardt optimization procedure. The obtained optimal parameters are given in the Tables III and IV, respectively.

Discussion

From the analysis of Table IV, a number of conclusions can be drawn.

Firstly, Eq. 8 corresponds well to the available experimental data within the entire investigated range of the discharge currents as the relative error of the experimental data approximation by this equation does not exceed 1%. Hence, the obtained experimental data prove that the reason of the sharp drop of the cells released capacity at the high discharge currents is the voltage drop at internal resistances of the cells.

Secondly, the currents i_0 and i_1 characterizing Eq. 8 depend not only on the capacity of the cells, but also on their design features, since for the cells from Table IV the ratios are $i_0/C_m = (1.821,$

Table II. Optimal values of parameters for Eq. 11 at discharge currents from Table I.

Model	CGR18650E	AMP20M1HDA	INR18650-13Q
C_{mref} (Ah)	2.25	20	1.338
Error ΔC_{mref} (Ah)	0.02	0.1	0.01
β	5.32	0.761	5.30
Error $\Delta\beta$	0.01	0.002	0.01
T_L (K)	237.0	235.5	236
Error ΔT_L (K)	0.6	0.5	0.6
K	1.03	1.142	1.033
Error ΔK	0.04	0.004	0.04
$\delta^{(a)}$ (%)	1.7	0.78	1.8

a) Relative error of experimental data approximation by Eq. 11 in Fig. 4.

7.875, 20.818) and $i1/C_m = (2.177, 19.344, 29.460)$ for cells CGR18650E, AMP20M1HDA, INR18650-13Q, respectively.

Thirdly, the relative error of experimental data approximation by the Eq. 8 (Table IV) is at least two times smaller than Eq. 3 (Table III), which does not take into account the internal resistance of the cells. Since the cells have internal resistance, therefore Eq. 3 should change its parameters $i0$ and n in such a way as to take into account the influence of internal resistance. Indeed, for Eq. 3 to take into account the influence of the internal resistance of cells at high discharge currents, it is necessary to increase (by absolute value) the slope angle specified by this equation at high currents (Fig. 5). For Eq. 3 according to the equation

$$\lim_{i \rightarrow i0} \frac{d}{di} C(i) = -C_m \frac{n}{4i0}, \quad [12]$$

this can be done by increasing the parameter n and decreasing the parameter $i0$. Comparing these parameters in Tables III and IV, we see that this is what actually happens. In this case, the coincidence of Eq. 3 with the experimental data will improve at high discharge currents, but worsen at medium and low discharge currents. As a result, the relative error of experimental data approximation by the Eq. 3 will be larger than Eq. 8, which explicitly takes into account the internal resistance of the cells. This conclusion corresponds to the found relative approximation errors for Eqs. 3 and 8 (Tables III and IV).

With use of the Eq. 8, it is possible to find the internal resistance of a cell

$$R = \frac{E - u_k - u_r}{i1}. \quad [13]$$

We evaluated the cell internal resistance with aid of the Eq. 13 and the found parameters ($i1$ from Table IV and u_k from Table I), as well as experimental values for EMF and relaxation polarizations u_r of the cells. However, experimental studies have shown that the parameters of EMF and u_r strongly depend on relaxation processes in the cells. In turn, relaxation processes depend on many factors: the design of the cells, the time of measurement of these parameters after the charge of the cells, temperature, the dispersion of the statistical parameters of the cells during their production etc. Therefore, before measuring the parameters, five initial cycles were performed to stabilize the accuracy of the charge (and, in particular, the CV phase) and the released capacity. Then, five more initial cycles were performed, in which four hours after charging the EMF of the cell was measured. The relaxation polarization u_r was found from the discharge curves according to Eq. 7. The data obtained were used to calculate the average values of these parameters and the absolute measurement errors. The absolute measurement error calculated by statistical methods takes into account both the accuracy of the measuring instruments used and the possible slight instability of the cell parameters.

As a result, it was obtained that the EMF of the charged LiFePO₄ cell is equal to $E = 3.56 \pm 0.01$ V, and the relaxation polarization is equal to $u_r = 0.25 \pm 0.01$ V. While the EMF of other cells is equal to $E = 4.17 \pm 0.01$ V, and relaxation polarization is equal to $u_r = 0.1 \pm 0.01$ V. The found values of the cell internal resistances are listed in the Table IV. It is interesting to note that the calculated cell internal resistances are close to the internal resistances of the same cells measured with aid of the alternating current with the frequency 1 kHz.

In conclusion, we note one important fact. For any batteries, a high enough current always exists, at which already at the battery discharge start, on its terminals, the voltage will be lower of the lower cutoff value, i.e. for such high current, the battery released capacity will be equal to zero. However at the present time, this fact is taken into consideration by neither the classical Peukert's equation nor any of its generalizations.²⁴

The lack of reflection of this experimental fact in modern equations, in our opinion, can be explained by two reasons.

Firstly, lithium-ion batteries are usually not used at such high discharge currents. Therefore, when developing analytical models of batteries operating under ordinary conditions, this region of discharge currents is not used at all (for example, in model,⁹ which calculates the remaining battery capacity, using the Peukert equation.). However, during the operation of any system using batteries, not standard situations are possible in which the discharge current may be close to or exceed the current $i1$ (at which $C(i1) = 0$). In this case, only the analytical models, that uses Eq. 8, and not Eqs. 1 or 3, can give the correct estimates.

Secondly, the majority of modern lithium-ion batteries has a small internal resistance, therefore, even at high discharge currents, the difference between Eqs. 3 and 8 is insignificant (for example, Samsung batteries—INR18650-13Q, see Fig. 5). Therefore, for these batteries, in the region of operating discharge currents, Eq. 3 and even Eq. 1 (Ref. 9) can be successfully used. However, some lithium-ion batteries (for example, Panasonic batteries—CGR18650E Table IV) and lithium-polymer batteries have internal resistance much bigger. Therefore, for analytical models of these batteries, it is necessary to use Eq. 8 rather than Eq. 3 or not to use these batteries at high discharge currents. For example, for a Panasonic battery—CGR18650E, even at currents greater than 2 C_n , Eq. 3 cannot be used (Fig. 5), and Eq. 1 cannot be used at currents greater than 0.9 C_n (Fig. 1).

Thus notwithstanding that the Eq. 3 corresponds quite well to the experimental data from most of the investigated lithium-ion battery types (for the usually used discharge currents for these batteries), however from the theoretical point of view, more correct is the Eq. 8. In addition, Eq. 8 must be used for all batteries with significant internal resistance.

Error Calculation for the Found Parameters

Studying various batteries, we were convinced that, despite all our efforts to stabilize the parameters of the batteries, a small

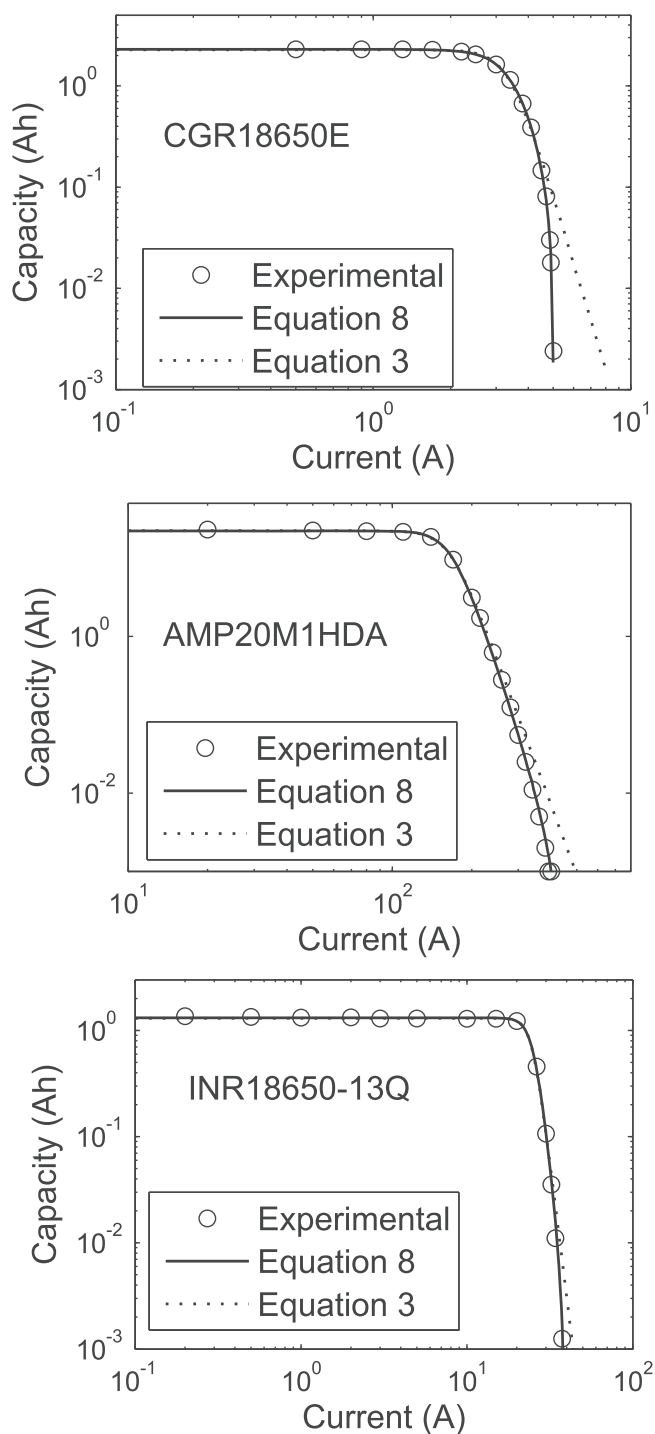


Figure 5. Comparison of generalized Peukert's Eqs. 3 and 8 with experimental data for capacity released by lithium-ion cells at various discharge currents in logarithmic system of coordinates.

dispersion of parameters always remains in the studied batteries. Therefore, when calculating the error of the found parameters, it is necessary to take into account not only the accuracy of the instruments, but also the inevitable dispersion of battery parameters. This can only be done by statistical methods.

In our experiments (Figs. 1, 4, 5), each experimental point was measured several times. This way, the error of each measured result (Figs. 1, 4, 5) could be calculated more accurately using statistical methods based on the obtained experimental results for each point of Figs. 1, 4 and 5. In this case, both the accuracy of the measuring

instruments used and the possible slight instability of the cell parameters were considered.

Optimal parameters in Tables II–IV were found based on the least square method with use of the Levenberg—Marquardt optimization procedure in the framework of a computer statistical program. When calculating the parameters, various estimates for the found parameters are calculated, such as: error, significance of the parameters, etc. Thus found errors are presented in Tables II–IV. It should be noted that when finding both optimal parameters and errors for these parameters, all the found values for the released capacity were used, and not only the average values at a certain current, which are presented in Fig. 5.

Conclusions

In conclusion, we note a number of advantages of the proposed generalized Peukert's Eq. 8 as compared to the classical Peukert's Eq. 1.

Firstly, the constants (i_0 and i_1) in Eq. 8 have the clear electrochemical sense unlike the classical Peukert's Eq. 1, where A is just an empiric constant.

Secondly, in the generalized Peukert's Eq. 8, the influence of the voltage drop, caused by the battery internal resistance, on the battery released capacity is taken into consideration. Consequently, a case is possible at the high discharge currents, that already at the moment of battery switch-on for discharge, on the battery terminals, the voltage will be less than the lower cutoff voltage. At these discharge currents, the capacity released by the battery will be zero. It should be noted that other generalizations of the Peukert equation do not take this experimental fact into account.

Thirdly, the generalized Peukert's Eq. 8 is applicable at any discharge currents including both very high and very small ones. In the classical Peukert's Eq. 1, the battery released capacity tends to infinity at discharge current decrease, which has no physical sense. Besides also as it was shown by the studies described in this paper, Eq. 1 is not applicable at the high discharge currents.

It should be noted that the generalized Peukert Eq. 3 is in good agreement with the experimental data for lithium-ion^{10,24} and nickel-cadmium²² batteries. Therefore, Eq. 8 should also correspond well to the experimental data for these batteries.

In addition, at low discharge currents, the classical Peukert Eq. 1 also corresponds well to experimental data (Fig. 1(1)). For modern batteries with low internal resistance (e.g. Samsung-INR18650-13Q) and for commercial automotive-grade lithium-ion batteries, the range of the discharge currents, where the classical Peukert Eq. 1 is applicable, covers the entire range of operating currents of these batteries. That is why in the Hausman's model,⁹ the classic Peukert equation (taking into account the temperature) is successfully used to estimate the remaining capacity of these batteries.

As for lead-acid and nickel-metal hydride batteries, the experimental data of these batteries better correspond to the classical Peukert Eq. 1 in a very wide range of discharge currents. This is especially evident at low discharge currents where Eqs. 3 and 8 are very poorly consistent with experimental data. However, since the released capacity of a battery of any type cannot be greater than the capacity that it received when charging, then at extremely low discharge currents the classical Peukert equation is also not applicable. At extremely low discharge currents for lead-acid batteries, the Liebenow Eq. 6 is used.²⁷ Nevertheless, the conducted experimental studies show that at very high discharge currents for any type of battery, any generalizations of the Peukert equation must take into account the internal resistance of the batteries.

Inasmuch the various generalizations of the Peukert's Eqs. 1, 3, 8 are widely used in diverse evaluations and models,^{9,10,28} the refinement of those equations and the ascertainment of the electrochemical mechanism on which they are based is of great practical and theoretical importance.

Table III. Optimal values of parameters for Eq. 3.

Model	CGR18650E	AMP20M1HDA	INR18650-13Q
C_m (Ah)	2.27	22.2	1.30
Error ΔC_m (Ah)	0.02	0.1	0.01
i_0 (A)	3.38	164.8	24.7
Error Δi_0 (A)	0.02	0.5	0.3
n	8.4	9.1	12.6
Error Δn	0.1	0.2	0.8
$\delta^{(a)}$ (%)	3.416	2.744	2.169

a) Relative error of experimental data approximation by the Eq. 3 in Fig. 5.

Table IV. Optimal values of parameters for Eq. 8.

Model	CGR18650E	AMP20M1HDA	INR18650-13Q
C_m (Ah)	2.301	22.2	1.32
Error ΔC_m (Ah)	0.002	0.1	0.01
i_0 (A)	4.19	174.8	27.4
Error Δi_0 (A)	0.01	0.5	0.2
n	5.41	8.9	10.4
Error Δn	0.05	0.2	0.7
i_1 (A)	5.01	429.3	38.8
Error Δi_1 (A)	0.01	0.8	0.4
$\delta^{(a)}$ (%)	0.166	0.971	0.941
R (m Ω)	213.55	3.1	40.5
Error ΔR (m Ω)	0.04	0.8	0.4

a) Relative error of experimental data approximation by the Eq. 8 in Fig. 5.

ORCID

N. E. Galushkin  <https://orcid.org/0000-0002-1613-8659>
 N. N. Yazvinskaya  <https://orcid.org/0000-0001-8147-8599>
 D. N. Galushkin  <https://orcid.org/0000-0001-8261-6527>

References

1. G. E. Blomgren, *J. Electrochem. Soc.*, **164**, A5019 (2017).
2. G. Zubi, R. Dufo-López, M. Carvalho, and G. Pasaoglu, *Renew. Sustain. Energy Rev.*, **89**, 292 (2018).
3. S. U. Kim, P. Albertus, D. Cook, C. W. Monroe, and J. Christensen, *J. Power Sources*, **268**, 625 (2014).
4. M. S. H. Lipu, M. A. Hannan, A. Hussain, M. M. Hoque, P. J. Ker, M. H. M. Saad, and A. Ayob, *J. Clean. Prod.*, **205**, 115 (2018).
5. M. A. Hannan, M. S. H. Lipu, A. Hussain, and A. Mohamed, *Renew. Sustain. Energy Rev.*, **78**, 834 (2017).
6. M. Cugnet, S. Laruelle, S. Grugeon, B. Sahut, J. Sabatier, J.-M. Tarascon, and A. Oustaloup, *J. Electrochem. Soc.*, **156**, A974 (2009).
7. H. Arunachalam, S. Onori, and I. Battiatob, *J. Electrochem. Soc.*, **162**, A1940 (2015).
8. G. Fan, K. Pan, M. Canova, J. Marcicki, and X. G. Yang, *J. Electrochem. Soc.*, **163**, A666 (2016).
9. A. Hausmann and C. Depcik, *J. Power Sources*, **235**, 148 (2013).
10. N. E. Galushkin, N. N. Yazvinskaya, and D. N. Galushkin, *J. Electrochem. Soc.*, **162**, A308 (2015).
11. O. Tremblay and L. A. Dessaint, *World Electr. Veh. J.*, **3**, 1 (2009).
12. N. E. Galushkin, N. N. Yazvinskaya, and D. N. Galushkin, *Int. J. Electrochem. Sci.*, **13**, 1275 (2018).
13. N. E. Galushkin, N. N. Yazvinskaya, and D. N. Galushkin, *Int. J. Electrochem. Sci.*, **9**, 6305 (2014).
14. N. E. Galushkin, N. N. Yazvinskaya, D. N. Galushkin, and I. A. Galushkina, *J. Electrochem. Soc.*, **161**, A1360 (2014).
15. N. E. Galushkin, N. N. Yazvinskaya, D. N. Galushkin, and I. A. Galushkina, *Int. J. Electrochem. Sci.*, **10**, 6645 (2015).
16. N. E. Galushkin, N. N. Yazvinskaya, and D. N. Galushkin, *Int. J. Hydrogen Energy*, **41**, 14813 (2016).
17. N. E. Galushkin, N. N. Yazvinskaya, and D. N. Galushkin, *J. Electrochem. Soc.*, **165**, A1303 (2018).
18. N. E. Galushkin, N. N. Yazvinskaya, and D. N. Galushkin, *J. Electrochem. Soc.*, **164**, A2555 (2017).
19. R. Jung, M. Metzger, F. Maglia, C. Stinner, and H. A. Gasteiger, *J. Electrochem. Soc.*, **164**, A1361 (2017).
20. M. Metzger, B. Strehle, S. Solchenbach, and H. A. Gasteiger, *J. Electrochem. Soc.*, **163**, A798 (2016).
21. N. E. Galushkin, N. N. Yazvinskaya, and D. N. Galushkin, *J. Electrochem. Soc.*, **166**, A897 (2019).
22. N. E. Galushkin, N. N. Yazvinskaya, D. N. Galushkin, and I. A. Galushkina, *Int. J. Electrochem. Sci.*, **9**, 4429 (2014).
23. C. Nebl, F. Steger, and H.-G. Schweiger, *Int. J. Electrochem. Sci.*, **12**, 4940 (2014).
24. N. E. Galushkin, N. N. Yazvinskaya, and D. N. Galushkin, *J. Electrochem. Soc.*, **167**, 013535 (2020).
25. W. Peukert, *Elektrotech. Z.*, **20**, 287 (1897).
26. C. M. Shepherd, *J. Electrochem. Soc.*, **112**, 657 (1965).
27. N. F. Compagnone, *J. Power Sources*, **35**, 97 (1991).
28. T. R. Crompton, *Battery Reference Book* (Newnes, Oxford) (2000).